# ATMOSPHERIC RESPONSE TO MODIFIED CLIMAP OCEAN BOUNDARY CONDITIONS DURING THE LAST GLACIAL MAXIMUM

E. Richard Toracinta[1], Robert J. Oglesby[3], and David H. Bromwich[1,2]
[1]Polar Meteorology Group, Byrd Polar Research Center, The Ohio State University
[2]Atmospheric Sciences Program, Department of Geography, The Ohio State University
[3]NASA Marshall Space Flight Center/National Space Science and Technology Center

## 1. INTRODUCTION

Although sea surface temperatures (SSTs) represent a critical lower boundary condition for global-scale paleoclimate simulations, the magnitude and distribution of SSTs at the Last Glacial Maximum (LGM), roughly 21,000 calendar years before present (21 kBP), remain uncertain. CLIMAP (Climate: Long-range Investigation, Mapping, and Prediction; CLIMAP 1981) produced the first systematic, global reconstruction of LGM SSTs. Relative to the present, the CLIMAP reconstruction shows annual mean cooling of less than 2°C throughout much of the equatorial Tropics and roughly the same magnitude of warming in the subtropical ocean gyres. Early global climate model (GCM) simulations of the LGM climate using the CLIMAP SSTs failed, however, to produce the magnitude of atmospheric cooling or change in the hydrologic cycle at low latitudes suggested by some terrestrial evidence (e.g., Rind and Peteet 1985).

Low-latitude LGM proxy data methods include alkenone-based estimates of tropical SSTs that show little change (e.g., Bard et al. 1997). In contrast, evidence from Barbados corals (Guilderson et al. 1994), snowline depressions (Rind and Peteet 1985), noble gases (e.g., Stute et al. 1992), pollen (Colinvaux et al. 1996), and tropical alpine glaciers (e.g., Thompson et al. 1995) indicates that LGM temperatures were 3-6°C cooler than today. Recent studies of sediment cores in the equatorial Pacific estimate cooling relative to present that is approximately 2°C greater than CLIMAP (e.g., Lea et al. 2000). Although a recent reassessment of the CLIMAP faunal data may have resolved some of the discrepancy with the proxy data (Crowley 2000), there is general agreement that the CLIMAP SSTs, particularly in the Tropics, are too warm.

At southern high latitudes, core analyses of diatom assemblages indicate a larger seasonal cycle of LGM circum-Antarctic sea ice extent than indicated by CLIMAP. Estimates of the LGM summer sea ice margin in specific sectors of the Southern Ocean vary, however, from the location of the modern winter extent (Gersonde and Zielinski 2000) to near the modern minimum (Crosta et al. 1998). Coupled ocean-atmosphere model results (e.g., Bush and Philander 1999) also indicate a much larger seasonal cycle of the Antarctic sea ice than predicted by CLIMAP. In the North Atlantic, SST estimates derived from sediment core analyses indicate that portions of the North Atlantic were relatively warm and at least seasonally ice free during the LGM (Hebbeln et al. 1994, among others). This prediction is corroborated by ocean surface circulation patterns inferred from foraminiferal assemblages in the northeast Atlantic (Lassen et al. 1999). Seasonally open water in the North Atlantic at the LGM has important implications for the Northern Hemisphere ice-sheet mass balance (Hebbeln et al. 1994).

Various methodologies have been employed to modify the prescribed ocean boundary condition for GCM paleoclimate simulations and resulting model temperature predictions show general agreement with proxy estimates (e.g., Rind and Peteet 1985; Yin and Battisti 2001). However, the previous studies are either regional in scope, focus primarily on the Northern Hemisphere climate, or do not include the effect of modified high latitude SSTs or sea ice. This paper presents results from two simulations of the LGM climate using the National Center for Atmospheric Research (NCAR) Community Climate Model version 3 (CCM3). The objective is to quantify the atmospheric response to a prescribed ocean boundary condition that is modified relative to CLIMAP, both in the Tropics and high latitudes, based on available proxy data. Section 2 describes the CCM3 and the LGM boundary conditions. Results from a CLIMAP (CL) simulation and an LGM simulation with modified SSTs (modCL) are presented and discussed in Section 3.

## 2. MODEL AND EXPERIMENTAL DESIGN

The NCAR CCM3 (Kiehl et al. 1998) is a global spectral atmospheric model with T42 truncation (2.8° lat. x 2.8° lon. transform grid), 18 hybrid sigma levels in the vertical, and a 20-minute time step. The CCM3 includes a fully interactive Land Surface Model (LSM; Bonan 1998) to evaluate surface fluxes of heat, moisture, and momentum.

Boundary conditions for the two LGM runs were identical except for the SSTs and sea ice extent. Laurentide, Fennoscandian, and Antarctic ice sheet and Patagonian ice cap elevations were implemented from glaciological model output (Johnson 2002; Hulton et al. 2002). Global sea level was lowered by 120 m commensurate with the LGM ice sheet volume. The solar forcing and trace gas concentrations were set to appropriate 21 kBP values. Present day vegetation was used in the simulations owing to the lack of a global LGM vegetation reconstruction.

Monthly mean SSTs for the CLIMAP run (CL hereafter) were derived by extrapolating the CLIMAP February and August data at each grid point to the

Corresponding author: Dr. E. Richard Toracinta, Byrd Polar Research Center, 1090 Carmack Road, The Ohio State University, Columbus, OH, 43210-1002. Email: toracinta.1@osu.edu

preserve the present day seasonal cycle. This approach is reasonable since present day and LGM solar forcing are very similar. Imposing the present day seasonal cycle results in only minor differences (< 0.5°C) in the SST annual and seasonal means in the Tropics (20°S–20°N). Fig. 1a shows the mean December–January–February (DJF) CL SSTs. Tropical SSTs are mostly 26°C or greater with the summer SSTs exceeding 28°C in the tropical Pacific Ocean. Sea ice (-1.8°C) extent shows little seasonal variability in the Southern Hemisphere. Seasonal changes in the Northern Hemisphere sea ice are also slight with greater seasonality in the sub-Arctic North Atlantic.

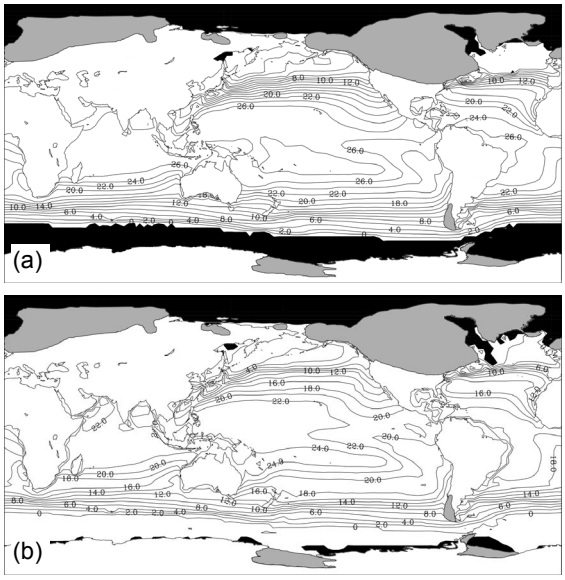


Fig. 1. Mean DJF SST for the (a) CL and (b) modCL LGM simulations. Contour interval is 2°C. Gray (black) shading indicates the ice sheet (mean sea ice) extent.

The SST boundary conditions for the modified CLIMAP run (modCL hereafter) were derived by first cooling the annual mean CL SSTs by 4°C in the tropical equatorial belt (30°N–30°S). From 30°–40° latitude, the SSTs were linearly interpolated to the annual mean CL SST values, with annual mean CL SSTs retained elsewhere. Next, the present day annual mean SST field was subtracted from the cooled annual mean CL SSTs and the difference field applied to each of the present day monthly mean SSTs to obtain the modCL SSTs. Thus, the magnitude of cooling in the modCL SSTs is related to the magnitude of cooling of the annual mean CL SSTs relative to present day. This method damps the CL seasonal cycle amplitude such that modCL DJF (JJA) SSTs are warmer (cooler) than CL. Figure 1b illustrates tropical cooling and reduced sea ice for the modCL run. In the Southern Hemisphere during DJF, sea ice retreats to near the Antarctic coast, similar to the modern condition. In the Northern Hemisphere, mean winter sea ice extent is similar for the two LGM runs. However, SSTs are somewhat warmer in the North Atlantic and North Pacific in the modCL distribution and the sea ice extent is reduced in mid to late winter (Jan/Feb) during the time of maximum extent (not shown).

Each model simulation was integrated for 18 years including a 3-year spin-up. Long-term annual and seasonal averages were computed from the monthly mean output.

## 3. RESULTS

The global annual mean 2-m temperature is 281.6 K in the CL run and 279.0 K in the modCL run. These are 4.5°C and 7.1°C colder, respectively, than the simulated present-day global annual mean 2-m temperature. The difference in mean 2-m temperature over the oceans alone for the modCL and CL runs (1.93°C) accounts for 75% of the difference in global mean 2-m temperature between the two runs. This is comparable to the fractional coverage of ocean area and shows that the cooling in the modCL global mean 2-m temperature relative to CL is largely due to the imposed SSTs. The global annual mean precipitation rate in the modCL run is 2.55 mm day$^{-1}$, which is a 12% (19%) reduction relative to CL (present day), respectively. LGM precipitation is reduced relative to present at all latitudes except the Southern Hemisphere low latitudes (10°S–25°S), due in part to increased precipitation along the South Pacific Convergence Zone (SPCZ) during the LGM as others have noted (e.g., Yin and Battisti 2001).

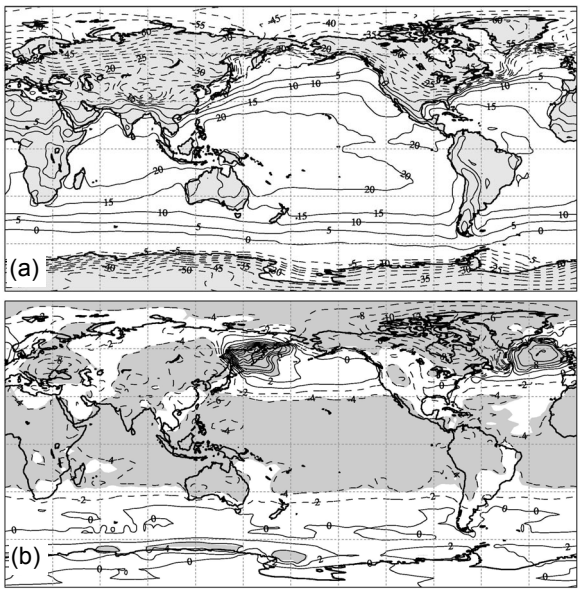


Fig. 2. 15-yr mean DJF 2-m air temperature for (a) modCL and (b) modCL minus CL. Contour interval is 5°C in (a) and 2°C in (b). Negative contours are dashed in (b) and shaded regions indicate statistical significance at the 99.9% level using Student's t-test.

The 15-year mean DJF modCL 2-meter air temperatures are shown in Fig. 2a with the differences relative to the CL run in Fig. 2b. In the Northern Hemisphere during DJF, positive 2-m temperature

anomalies exceed 12°C over the North Atlantic and 20°C over the Sea of Okhotsk in eastern Russia (Fig. 2a). During JJA, the anomalies exceed 8°C over portions of the South Pacific (not shown). These are due primarily to the prescribed SSTs. For example, in the western North Pacific, the modCL SSTs are 1–4°C warmer through the boreal winter months resulting in less extensive sea ice and greater fluxes of sensible and latent heat (50-100 W $m^{-2}$) to the lower troposphere relative to CL. This phenomenon also occurs in the high latitude ocean basins during summer, although the 2-m temperature anomalies are smaller in magnitude than in winter.

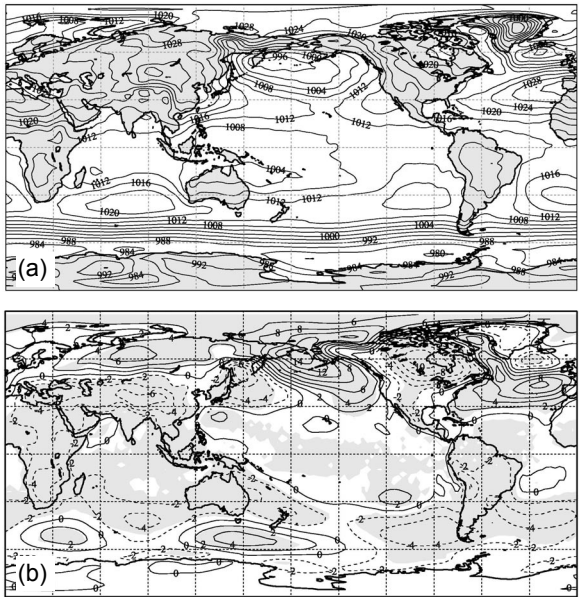


Fig. 3. 15-yr mean DJF MSLP for (a) modCL and (b) modCL minus CL surface pressure difference. Contour interval is 4 hPa in (a) and 2 hPa in (b).

The 2-m temperature anomalies over the high latitude oceans significantly impact the atmospheric mass field. Figure 3a shows the DJF mean sea level pressure (MSLP) for the modCL run with the surface pressure difference relative to CL in Fig. 3b. In the modCL run, the Aleutian low in the North Pacific is located westward of its position in the CL run. The surface pressure anomalies show large (> 8 hPa) pressure decreases over the Sea of Ohkotsk with pressure increases in the central and eastern North Pacific. The anomaly pattern results from thermal gradients having opposing effects. The decreased meridional SST gradient in the modCL run results in a general weakening of the wintertime Aleutian low except in the western North Pacific where the juxtaposition of relatively warm temperatures over the Sea of Ohkotsk and cold continental temperatures increases the local baroclinicity. A similar phenomenon occurs over the North Atlantic in winter, resulting in a stronger Icelandic low in the modCL run (Fig. 3b).

In the Southern Hemisphere, the DJF surface pressure anomalies along the westerly wind belt resemble a wave number two pattern (Fig. 3b). The anomalies are the result of weaker (2-4 hPa) subtropical high pressure centers and a relaxed meridional pressure gradient due to the reduced meridional temperature gradient in the modCL run.

At upper levels, comparison of the 500-hPa geopotential height fields for the two LGM runs indicates a weaker midlatitude atmospheric circulation in the modCL simulation (not shown). The changes occur in both hemispheres and during both extreme seasons, but are most pronounced in the winter hemisphere. Pronounced positive and negative DJF 500 hPa height anomalies are located over the North Atlantic, North Pacific, and the Laurentide Ice Sheet. The Northern Hemisphere anomaly pattern is due to a westward shift and slight deamplification of the modCL 500-hPa longwave pattern. The westward shift of the mid-tropospheric longwave pattern is a dynamic response to the low-level thermal anomalies over the Sea of Okhotsk and western North Pacific. The modCL surface pressure and 500-hPa height anomalies, from the Sea of Okhotsk to the Bering Strait, are very similar to the atmospheric Rossby wave response to anomalous thermal forcing noted in the contemporary environment (Honda et al. 1999).

The deamplification of the 500-hPa longwave pattern directly affects the precipitation accumulation over the continental ice sheets (not shown). During DJF, precipitation in the modCL simulation is significantly reduced relative to CL over the central and eastern Pacific and much of North America. Likewise, significant precipitation decreases occur across the North Atlantic except in the vicinity of the intensified Icelandic low. In the Southern Hemisphere, precipitation is decreased significantly over the circumpolar oceans during summer and winter (not shown), consistent with the weaker midlatitude atmospheric circulation. At low latitudes in the modCL run, significant precipitation decreases occur during DJF over much of the Tropics with the exception of Amazonia and the tropical North Atlantic, the SPCZ region, the Hawaiian Islands, southeastern Africa, and the western Indian Ocean. The distribution of low-latitude precipitation anomalies generally agrees with regions identified by Ropelewski and Halpert (1989) with statistically significant precipitation-cold phase El Niño/Southern Oscillation relationships.

Pronounced regional-scale changes also occur in the Northern Hemisphere monsoon circulation due to an increased land/ocean temperature difference in the modCL run. During JJA, negative surface pressure anomalies (2-6 hPa) occur over Asia with small positive anomalies in the Indian Ocean (not shown). Consequently, the cross equatorial near-surface flow is increased in the region with the Somali jet nearly 50% (7 m $s^{-1}$) stronger in the modCL run. The enhanced low-level monsoon flow is accompanied by increased precipitation, which has a direct impact on the mean meridional circulation. Driven largely by Asian monsoon convection and latent heat release, the JJA Southern Hemisphere Hadley cell is approximately 20% more intense than in CL. Elsewhere, the mean meridional circulation cells are weaker in the modCL run indicating that the increased land/ocean

temperature contrast primarily affects the Asian monsoon region.

Quantitative estimates of LGM surface temperature are available from a large number of proxy sources for comparison with the model predicted annual mean temperature. The mean temperature anomalies for 54 proxy locations grouped by land/ocean and by latitude belt are given in Table 1. Averaged by latitude in the Tropics and subtropics, the modCL results overestimate the LGM cooling, but are closer than CL to proxy temperature estimates. In mid- and high latitudes (poleward of 40$^{o}$), the modCL results are in close agreement with proxy estimates, suggesting that warmer high latitude SSTs and reduced sea ice at the LGM indicated by some proxy sources (e.g., Crosta et al. 1998) was an important modulator of LGM climate.

Table 1. Mean surface temperature difference (LGM minus present; $^{o}$C) from proxy estimates and CCM3 output. The data sample sizes are in parentheses.

| | All (54) | Land (31) | Ocean (23) |
|---|---|---|---|
| Proxy | -5.8 | -7.8 | -3.2 |
| modCL | -6.9 | -8.3 | -5.0 |
| CL | -3.5 | -4.8 | -1.7 |

| | By Latitude | | |
|---|---|---|---|
| | 20$^{o}$N–20$^{o}$S (24) | 20$^{o}$–40$^{o}$ (13) | > 40$^{o}$ (17) |
| Proxy | -4.1 | -4.8 | -9.1 |
| modCL | -5.8 | -6.4 | -8.9 |
| CL | -1.3 | -2.7 | -7.1 |

Efforts to reconcile land and ocean temperature estimates from LGM proxy data have been ongoing for nearly 25 years. Feldberg and Mix (2002) comment that it may be appropriate to apply estimates of LGM cooling on a regional rather than global scale. Our LGM results suggest that, while some regional tuning may be necessary, uniform SST cooling at low latitudes and modifications to high latitude sea ice are sufficient to capture to first approximation the regional and synoptic-scale climate over much of the globe at the LGM.

**ACKNOWLEDGMENTS.** This project is sponsored by NSF grant OPP-9905381 to D. H. Bromwich. Use of computer resources at NCAR and the Ohio Supercomputing Center was provided through grants 36091009 and PAS0045-1, respectively.

**REFERENCES**

Bard, E., F. Rostek and C. Sonzogni, 1997: Interhemispheric synchrony of the last deglaciation inferred from alkenone palaeothermometry. *Nature*, **385**, 707-710.

Bonan, G.B., 1998: The land surface climatology of the NCAR Land Surface Model Coupled to the NCAR Community Climate Model. *J. Climate*, **11**, 1307-1326.

Bush, A.B.G. and S.G.H. Philander, 1999: The climate of the Last Glacial Maximum: Results from a coupled atmosphere-ocean general circulation model. *J. Geophys. Res.*, **104**, 24509-24525.

CLIMAP Project Members, 1981: *Seasonal Reconstruction of the Earth's Surface at the Last Glacial Maximum.* Geol. Soc. Amer. Map and Chart Series, Vol. 36, 18.

Colinvaux, P.A., P.E. Deoliveira, J.E. Moreno, M.C. Miller and M.B. Bush, 1996: A long pollen record from lowland amazonia: Forest and cooling in glacial times. *Science*, **274**, 85-88.

Crosta, X., J.-J. Pichon and L.H. Burckle, 1998: Reappraisal of Antarctic seasonal sea-ice at the Last Glacial Maximum. *Geophys. Res. Lett.*, **25**, 2703-2706.

Crowley, T.J., 2000: CLIMAP SSTs re-revisited. *Climate Dyn.*, **16**, 241-255.

Feldberg, M.J. and A.C. Mix, 2002: Sea-surface temperature estimates in the Southeast Pacific based on planktonic foraminiferal species; modern calibration and Last Glacial Maximum. *Marine Micropaleon.*, **44**, 1-29.

Gersonde, R. and G. Zielinski, 2000: The reconstruction of late Quaternary Antarctic sea-ice distribution - the use of diatoms as a proxy for sea-ice. *Palaeogeog., Palaeoclim., Palaeoecol.*, **162**, 263-286.

Guilderson, T.P., R.G. Fairbanks and J.L. Rubenstone, 1994: Tropical temperature variations since 20,000 years ago: Modulating interhemispheric climate change. *Science*, **263**, 663-665.

Hebbeln, D., T. Dokken, E.S. Andersen, M. Hald and A. Elverhøi, 1994: Moisture supply for northern ice-sheet growth during the Last Glacial Maximum. *Nature*, **370**, 357-360.

Honda, M., K. Yamazaki, H. Nakamura and K. Takeuchi, 1999: Dynamic and thermodynamic characteristics of atmospheric response to anomalous sea-ice extent in the Sea of Okhotsk. *J. Climate*, **12**, 3347-3358.

Hulton, N.R.J., R.S. Purves, R.D. McColloch, D.E. Sugden and M.J. Bentley, 2002: The Last Glacial Maximum and deglaciation of southern South America. *Quat. Sci. Rev.*, **21**, 233-241.

Johnson, J.V., 2002: *A basal water model for ice sheets*. Ph.D. dissertation, University of Maine, 200 pp.

Kiehl, J.T., J.J. Hack, G.B. Bonan, B.A. Boville, D.L. Williamson and P.J. Rasch, 1998: The National Center for Atmospheric Research Community Climate Model: CCM3. *J. Climate*, **11**, 1131-1149.

Lassen, S., E. Jansen, K.L. Knudsen, A. Kuijpers, M. Kristensen and K. Christensen, 1999: Northeast Atlantic sea surface circulation during the past 30-10 $^{14}$C kyr B.P. *Paleocean.*, **14**, 616-625.

Lea, D.W., D.K. Pak and H.J. Spero, 2000: Quaternary equatorial Pacific sea surface temperature variations. *Science*, **289**, 1719-1724.

Rind, D. and D. Peteet, 1985: Terrestrial conditions at the Last Glacial Maximum and CLIMAP sea-surface temperature estimates: Are they consistent? *Quat. Res.*, **24**, 1-22.

Ropelewski, C.F. and M.S. Halpert, 1989: Precipitation patterns associated with the high index phase of the Southern Oscillation. *J. Climate*, **2**, 268-284.

Stute, M.,P. Schlosser, J.F. Clark and W.S. Broecker, 1992: Paleotemperatures in the southwestern United States derived from noble gases in ground water. *Science*, **256**, 1000-1003.

Thompson, L.G., E. Mosley-Thompson, M.E. Davis, P.-N. Lin, K.A. Henderson, J. Cole-Dai, J.F. Bolzan and K.-b. Liu, 1995: Late Glacial Stage and Holocene tropical ice core records from Huascarán, Peru. *Science*, **269**, 46-50.

Yin, J.H. and D.S. Battisti, 2001: The importance of tropical sea surface temperatures patterns in simulations of Last Glacial Maximum climate. *J. Climate*, **14**, 565-581.